

# Broadband refocusing pulses with $B_1$ robustness and energy constraints

M. A. Janich<sup>1,2</sup>, R. F. Schulte<sup>2</sup>, M. Schwaiger<sup>3</sup>, and S. J. Glaser<sup>1</sup>

<sup>1</sup>Chemistry, Technische Universität München, Munich, Germany, <sup>2</sup>GE Global Research, Munich, Germany, <sup>3</sup>Nuclear Medicine, Technische Universität München, Munich, Germany

## Introduction

Broadband refocusing pulses are of great interest in localized spectroscopy for improving spatial selectivity, reducing chemical-shift displacements, and reducing anomalous  $J$  modulation. In practice the bandwidth of amplitude modulated pulses is limited by the maximum  $B_1$  amplitude produced by the RF coil. Broad bandwidth is achieved by amplitude and phase modulated pulses designed with the Shinnar-Le Roux algorithm (SLR) [1], optimal control theory (OCT) [2], or with adiabatic pulses [3]. This work extends the OCT approach to limiting pulse energy, which can be necessary under constraints of specific absorption rate (SAR). Slice-selective Broadband Universal rotation By Optimized Pulses (S-BUBOP) are compared to broadband SLR pulses (BB-SLR) and verified experimentally in the PRESS sequence.

## Methods

RF pulses are optimized with a gradient ascent algorithm [4]. The quality function drives the RF pulse to  $180^\circ$  universal rotation of spins in the pass-band and prevention of excitation in the stop-band [2]. Immunity against  $B_1$  variation is obtained by optimizing for a range of discrete  $B_1$  offset values [5]. The cases of exact  $B_1$  calibration (S-BUBOP-0%), and deviations  $\pm 10\%$  (S-BUBOP-10%) and  $\pm 20\%$  (S-BUBOP-20%) are considered. The pulse is optimized under two limitations: at each iteration of the algorithm, the pulse is truncated at the amplitude limit  $B_{1max}$  and scaled to  $B_1(n) \rightarrow B_1(n) \cdot \sqrt{E_{max}/E}$ , if it exceeds the energy limit ( $E > E_{max}$ ) [6]. Pulse energy is calculated according to  $E \sim T/N \sum_{n=1}^N |B_1(n)|^2$ , with  $T$  being pulse duration.

Exemplary pulses with the following specifications are optimized: time-bandwidth product  $TBW=17.4$ , fractional transition width  $FTW=0.18$ , ratio of pulse bandwidth to peak  $B_1$  amplitude  $BW/B_{1max}=2.95$ . For a scaling of  $B_{1max}=23\mu T$  (1kHz for  $^1H$ ), these pulses have  $BW=2950Hz$  and  $T=5.9ms$ . These specifications correspond to the BB-SLR pulse with  $nbw=110$  from [1], with the exception of  $180^\circ$  rotation instead of  $172^\circ$ . Pulse energies are given relative to a conventional, amplitude modulated SLR pulse with  $TBW=4$ ,  $FTW=0.43$ ,  $BW/B_{1max}=0.95$ . PRESS experiments on a phantom with oil and water are performed on a 3T GE Signa HDx using a head T/R coil.

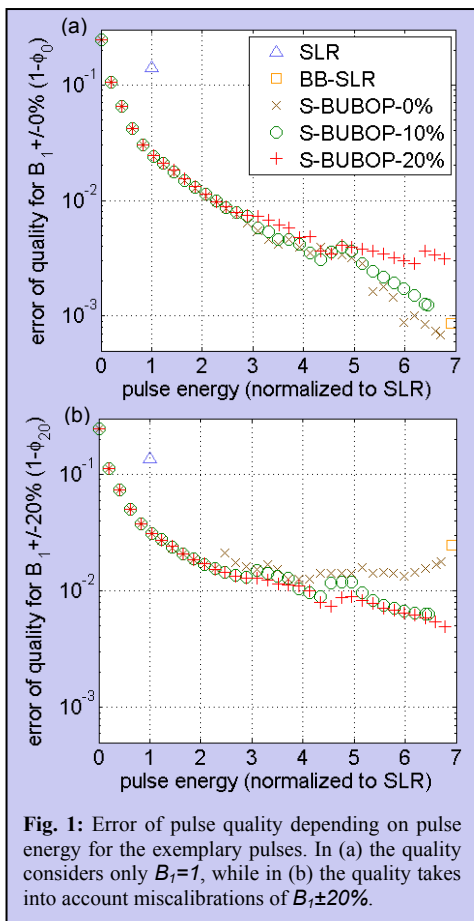


Fig. 1: Error of pulse quality depending on pulse energy for the exemplary pulses. In (a) the quality considers only  $B_1=1$ , while in (b) the quality takes into account miscalibrations of  $B_1 \pm 20\%$ .

miscalibration of 20% the BB-SLR shows signal loss, while S-BUBOP-20% performs well (Fig. 2h).

## Conclusions

Broadband pulses generally require more energy than non-broadband pulses. Compared to a standard SLR pulse, the exemplary S-BUBOP-20% pulse increases the bandwidth by a factor of 3 using a factor of 4.5 larger pulse energy, and with a smaller transition zone. Unlike BB-SLR pulses, S-BUBOP are robust against  $B_1$  miscalibrations.

**Acknowledgement:** This work was partly funded by BMBF MOBITUM grant #01EZ0826/7.

**References:** [1] Schulte RF et al. JMR 190:271 (2008); [2] Janich et al. ISMRM 2860 (2010); [3] Garwood et al. JMR 153:155 (2001); [4] Khaneja N et al. JMR 172:296 (2005); [5] Kobzar K et al. JMR 173:229 (2005); [6] Kobzar K et al. JMR 194:58 (2008)

## Results and Discussion

Optimizations are performed for different energy limits, while keeping  $T$ ,  $BW$ ,  $FTW$ , and  $B_{1max}$  fixed. This gives a curve of pulse quality for different pulse energies. Error of quality is plotted against pulse energy, using the quality function for exact  $B_1$  calibration (Fig. 1a) and with  $B_1$  miscalibration of  $\pm 20\%$  (Fig. 1b). The standard SLR pulse with the same  $B_{1max}$  is given for comparison. Its quality is low because it is not broadband.

The quality increases with larger pulse energy. Pulses optimized without considering  $B_1$  deviations (S-BUBOP-0%) reach a slightly better quality with slightly less energy compared to BB-SLR (see cross and square in Fig. 1a). For the same energy, pulses optimized with robustness against  $B_1$  inhomogeneity perform worse for exact  $B_1$  calibration (see circle and plus sign in Fig. 1a), compared to S-BUBOP-0%. For the same quality, pulses with better  $B_1$  robustness need more energy.

When looking at pulse performance under  $B_1 \pm 20\%$  the BB-SLR pulse and S-BUBOP-0% pulses perform worse (see cross and square in Fig. 1b). Optimizing for  $B_1 \pm 10\%$  gives good robustness against  $B_1 \pm 20\%$ . For  $B_1 \pm 20\%$  the best pulse quality of 0.995 is reached with relative pulse energy of 6.8.

In a PRESS experiment the S-BUBOP-20% pulse with energy 4.5 is compared to SLR and BB-SLR (Fig. 2). The chemical-shift displacement between oil and water resonances is reduced with S-BUBOP-20% and BB-SLR (Fig. 2g). With a  $B_1$

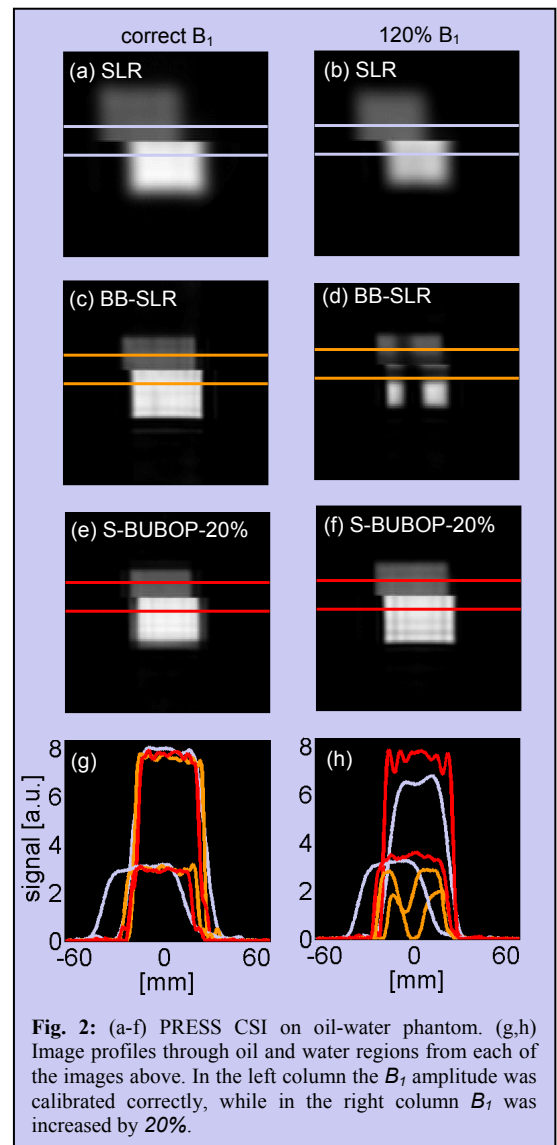


Fig. 2: (a-f) PRESS CSI on oil-water phantom. (g,h) Image profiles through oil and water regions from each of the images above. In the left column the  $B_1$  amplitude was calibrated correctly, while in the right column  $B_1$  was increased by 20%.